Near-field optical scanning microscopy with tunnel-distance regulation

by Urs Dürig
Dieter Pohl
Flavio Rohner

Unprecedented optical image resolution (20 nm to 30 nm) has been obtained with a near-field optical scanner using light with a wavelength of half a micrometer. The key element is an extremely small aperture (~10 nm) placed at the very top of a pyramidal screen. The aperture is scanned in the immediate proximity of the surface to be investigated, using vacuum tunneling to sense the distance. The amount of light transmitted by both the aperture and the sample depends sensitively on the optical properties of the sample in the immediate vicinity of the aperture.

1. Introduction

The concept of near-field optical scanning (NFOS) microscopy [1, 2] is closely related to scanning tunneling microscopy (STM). Both methods use a local probe scanned in the immediate proximity of a sample surface to acquire information with high spatial resolution. A crucial point for the recording of reproducible, high-resolution NFOS micrographs is the use of vacuum tunneling as a servo-mechanism to maintain the optical probe in close contact with the sample without actually touching it.

The resolution in any imaging process is restricted by diffraction to approximately $2\pi/q_{max}$, where q_{max} is the largest wave number of the Fourier components contributing to the image. This very basic law of physics is directly related to Heisenberg's uncertainty principle. In conventional microscopy, q_{max} is limited to $2/\lambda$, resulting in an ultimate resolution of the order of 200 to 300 nm for λ in the visible region. However, the upper bound on q_{max} can be increased by orders of magnitude if the additional information contained in an optical near field is exploited. The acoustic analog of this scheme is the medical doctor's stethoscope, which achieves a resolution better than $\lambda/100$.

In our experiments on NFOS microscopy, an aperture in an opaque metallic screen acts as a submicroscopic light source that is scanned across the sample surface, and the intensity of the light transmitted through the sample is recorded. A simple technique of aperture production described in the next section enabled us to develop the first workable microscope within a short time [2, 3]. With this microscope, objects 20 to 30 nm in size could be clearly recognized using 488-nm radiation. This corresponds to a resolution of the order of $\lambda/20$. To obtain such high resolution, the aperture has to be maintained at a distance of less than 10 nm from the sample surface, and its diameter must not exceed 20 nm.

The electromagnetic near field at the aperture may be thought of as being a superposition of evanescent waves which are scattered by the sample. In terms of Fourier optics [4] it can be shown that the amplitude of these scattered waves is proportional to the optical density of the sample averaged over the aperture area, provided the sample is thin compared to the aperture dimensions. Also, the distance between aperture and sample must not exceed this limit; otherwise the short-wavelength Fourier components of the near field are strongly damped when arriving at the sample. The resolution becomes correspondingly poorer with increasing distance.

In 1972, E. A. Ash and G. Nichols [5] demonstrated near-field imaging for the first time using 3-cm microwave radiation. Lewis et al. analyzed the requirements for optical near-field microscopy in 1983 [6]. The authors demonstrated, in particular, light transmission through arrays of submicroscopic apertures and its variation with aperture size. Massey [4] independently suggested NFOS microscopy on the basis of theoretical considerations. This work was very recently supplemented by an experimental study [7] using far-infrared radiation. Fischer [8], using a concept somewhat different from ours, recently demonstrated an interesting attempt directed towards NFOS reflection microscopy.

2. NFOS design

- *Submicroscopic aperture*

Only a tiny fraction of the incident intensity is scattered by a submicroscopic aperture. Therefore, the metal screen containing the aperture must have a thickness at least an order of magnitude larger than the skin depth to prevent excessive stray radiation. Conversely, the screen thickness should not exceed aperture dimensions, else the transmissivity of the aperture acting as an overdamped waveguide would be too small. A tapered wall hole [**Figure 1(a)**] best reconciles the conflicting requirements of maximum film thickness and minimum aperture diameter.

The boundary of the resulting aperture is not sharp. An effective radius a_{eff} can be defined in terms of the radius of curvature r_k and the skin depth d_p,

$$a_{eff} = d_p\sqrt{1 + r_k/d_p}; \tag{1}$$

d_p is given by the extinction coefficient of the metal κ and the wavelength λ:

$$d_p = \frac{\lambda}{4\pi\kappa}. \tag{2}$$

The smallest aperture radius is 6 nm for aluminum coverage $[r_k = 0, \kappa \sim 6]$.

The aperture is placed at the very apex of a strongly pointed tip. By this means, the aperture can be brought close to the object to be imaged even if the sample surface is corrugated. In our setup, we use quartz tips with a cross section of 2×2 mm^2 and a length of about 8 mm [**Figure 1(b)**]. The radius of curvature at the apex, sharpened by ion-milling or anisotropic etching, is less than 10 nm. The whole quartz tip is covered with an opaque 1000-nm aluminum film except for the base plane where the incident light enters.

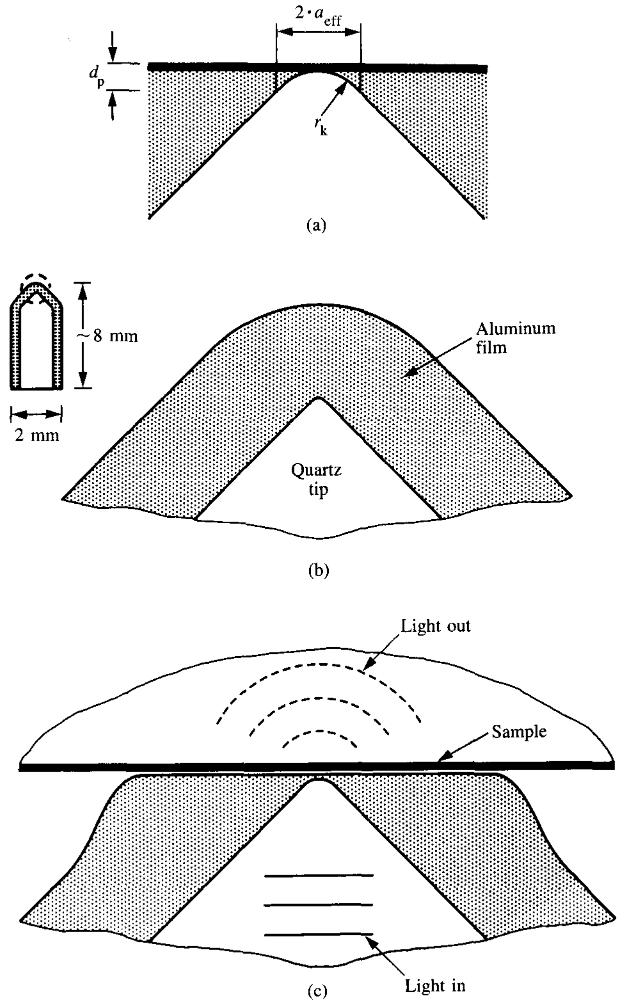

Figure 1

(a) Tapered wall hole. (b) Quartz tip smoothly covered with an opaque aluminum film before aperture formation. (c) End phase of aperture formation.

The aperture at the apex is formed by pressing the tip against a transparent part of the sample surface (usually a microscope slide), thereby flattening and thinning the metal film which smoothly surrounded the apex before [see **Figure 1(c)**]. This cold deformation process is continued until faint light emission from the apex is seen. The procedure is self-aligning with respect to apex position and very simple. However, the lifetime of the aperture is limited to a few hours during which the diameter grows slowly, probably due to internal stress created in the metal film during aperture

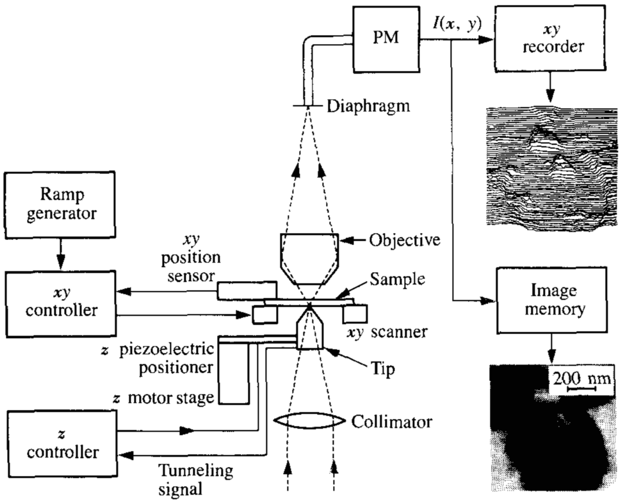

Figure 2

Schematic diagram of NFOS microscope. A high-resolution NFOS micrograph and the corresponding line scan are shown at right.

formation. Moreover, the yield in apex sharpening is fairly poor. Both lifetime and yield have to be improved for more routine high-resolution NFOS work.

• *Overall instrument*

The NFOS microscope setup, sketched in **Figure 2**, is mounted on top of a vibration-damped honeycomb table. The beam of an argon laser (Coherent Model 53, $\lambda = 488$ nm), cleaned and expanded by a filter/telescope combination, is focused onto the aperture at the apex of the quartz tip by means of a finely adjustable lens ($f = 50$ mm). The tip is mounted on a vertical translator consisting of a motor-driven micrometer stage for coarse adjustment and a z piezoelectric positioner which permits control of the aperture-to-sample distance in the nanometer range. A large displacement capability of 0.15 μm/V and adequate mechanical stiffness (lowest resonance at approximately 350 Hz) are obtained by using a pair of coupled bimorphs [9] **[Figure 3(a)]**.

Distance control between aperture and sample in the nanometer range is crucial for the operation of the NFOS microscope. Conventional methods such as sensing electrical or physical contact can be used, but in our experience *tunnel-distance regulation* is far superior to these more conventional methods, provided the sample is at least slightly conducting. The most important advantages are increased scanning speed and avoidance of direct physical contact between the delicate tip and the sample surface.

Microscopic protrusions on the flattened metal layer at the apex can act as tunneling tips. Typically, a voltage of 500 mV is applied between tip and sample and the tunneling current is stabilized to 1 nA by a feedback amplifier acting on the z positioner described above. The small distance maintained in this way ensures that the sample dives into the near-field zone of the aperture during NFOS operation **[Figure 4]**.

The sample is mounted on an xy table, as shown in **Figure 3(b)**. Its base is attached to a conventional micrometer xy stage for rough alignment (not shown in the figure). Two pairs of bimorphs provide motion in the x and y directions. The scan range is 50×50 μm^2 with a voltage sweep of 120 V. The lowest resonance of this unit occurs at a frequency of roughly 100 Hz, and it has a Q factor of the order of 20.

The lateral position of the sample is measured optically by means of a quadrant detector firmly attached to the mounting base of the tip translator stage, plus the LED and pinhole assembly also shown in Figure 3(b). By using feedback amplifiers which actuate the xy piezoelectric scanner, it is possible to eliminate creep and hysteresis to a high degree of precision. The short-term stability of this simple system is at least 5 nm **[Figure 3(c)]**.

The relatively high Q of the first resonance of the scanner limits the loop bandwidth to a maximum of 5 Hz and also prohibitively increases sensitivity to external vibrations at the resonance frequency. Performance can be improved considerably by applying an additional feedback signal proportional to the time derivative of the measured position. Thereby, the resonance and the lateral vibrations of the sample relative to the tip are effectively damped. At the same time, the bandwidth of the feedback loop can be increased by a factor of 10.

The light transmitted through both aperture and sample is collected by a microscope (objective: 40×, numerical aperture = 0.6) as indicated in Figure 2. It falls upon the end of a fiber cable which directs the radiation to a photomultiplier (PM). A diaphragm in the image plane eliminates stray light resulting, for instance, from imperfections in the metal coverage of the quartz tip. The microscope also permits visual inspection of the sample, which is important, in particular, during alignment of the instrument.

The output of the photomultiplier is sent simultaneously to an xy recorder and into an analog image memory (Princeton Electronic Products, Model 500). Thus, line-scan graphs as well as gray-scale pictures of TV quality have been obtained.

3. Results

A number of test slides were scanned with the NFOS microscope to study its imaging capabilities. The samples were microscope slides covered with thin metal films containing patterns of transparent grooves and circular holes. Additionally, 10 nm of gold–antimony alloy (99%/1%) was sputtered onto the samples to ensure the good electrical conductivity needed for distance regulation. In

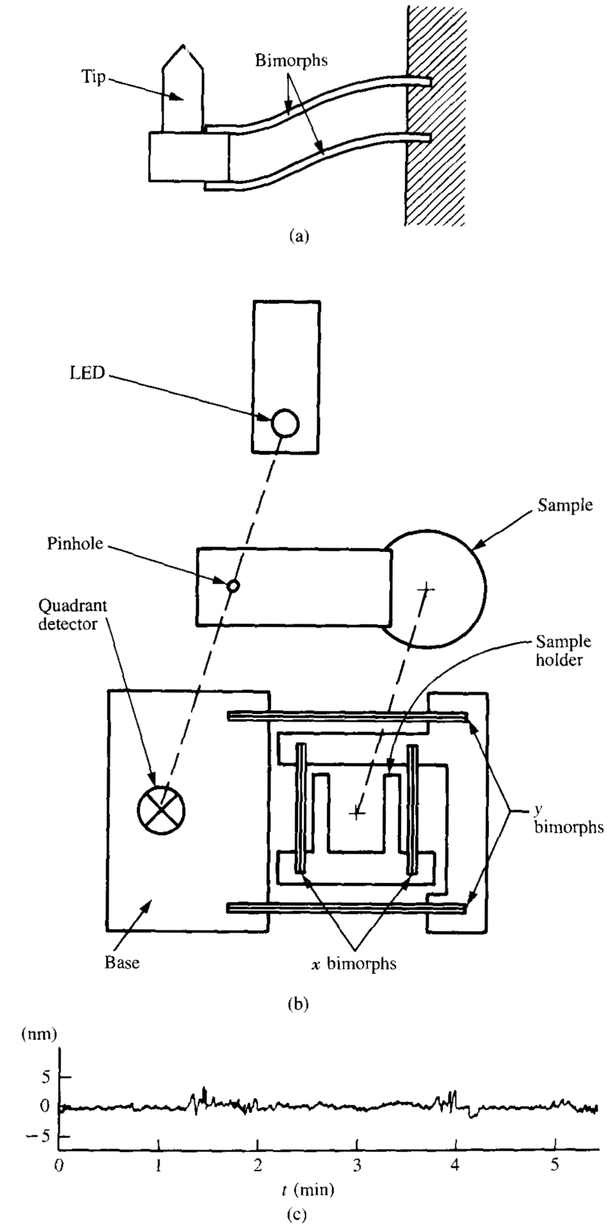

Figure 3

(a) z positioner and (b) xy scanner with position sensor (exploded view). From *Proceedings*, 29th Annual International Technical Symposium on Optical and Electro-Optical Engineering, San Diego, CA, August 1985; ©The Society of Photo-Optical Instrumentation Engineers, reprinted with permission. (c) Residual vibrations of the xy scanner with feedback turned on.

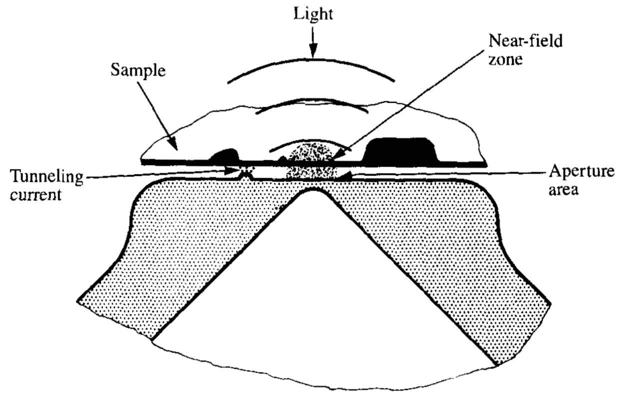

Figure 4

Aperture held at operating distance by means of tunneling.

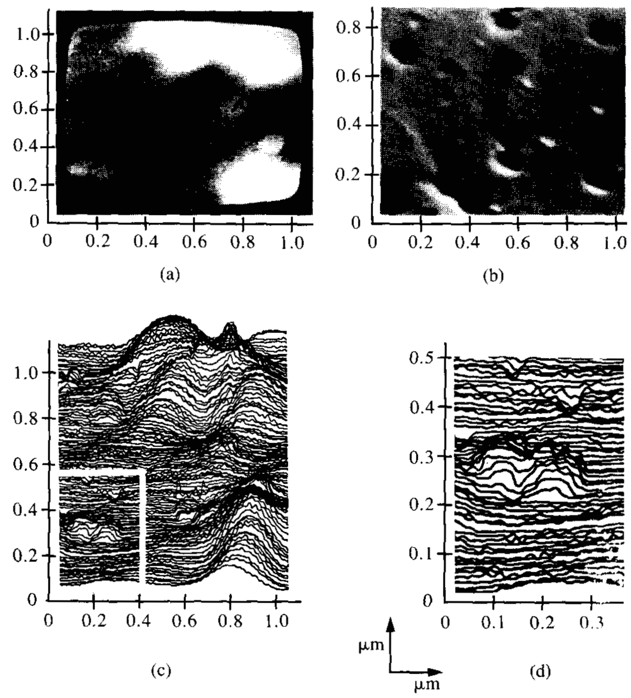

Figure 5

(a) High-resolution NFOS micrograph of a 30-nm Ta film with 100-nm holes. (b) SEM micrograph of the same sample. (c) Line-scan record of the transmitted intensity corresponding to (a). (d) Magnification of the inset. (a), (b), and (c) from *Proceedings*, 29th Annual International Technical Symposium on Optical and Electro-Optical Engineering, San Diego, CA, August 1985; ©The Society of Photo-Optical Instrumentation Engineers, reprinted with permission.

general, the aperture at the apex was formed immediately before performing a measurement, using a transparent zone of the actual test slide as a counterpiece.

Strong interferences of the transmitted intensity with a period $\lambda/2$ are observed as the aperture approaches the sample. The intensity has a last minimum at a distance of typically 30 nm above the surface, and it rises to about 10%

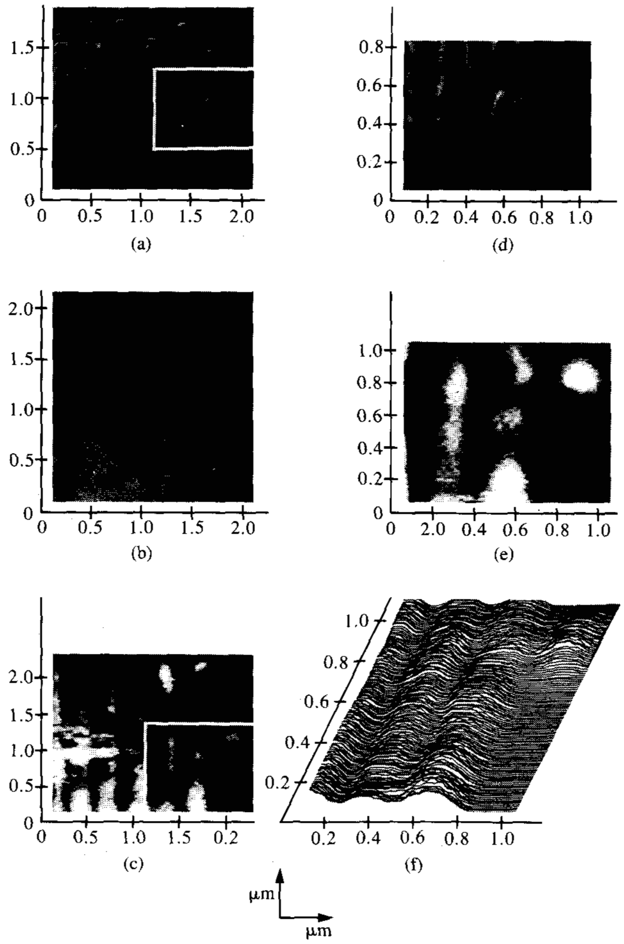

Figure 6

(a) SEM, (b) conventional optical, and (c) medium-resolution NFOS micrographs of the same area of a transparent 400-nm periodicity line-grating structure in a chromium film. (d) and (e) magnifications of the insets in (a) and (c), respectively. (f) Line scan corresponding to (e). (a), (b), and (c) from *Proceedings*, 29th Annual International Technical Symposium on Optical and Electro-Optical Engineering, San Diego, CA, August 1985; ©The Society of Photo-Optical Instrumentation Engineers, reprinted with permission.

of its maximum at working distance. This increase is a consequence of the finite reflectivity of the sample surface.

Areas of either 1 μm × 1 μm or 2.5 μm × 2.5 μm were usually scanned. Recording a full image comprising 128 lines took about ten minutes. The speed was primarily limited by the response time of the distance regulation.

NFOS micrographs of two different samples are presented here. They demonstrate the maximum attainable resolution, imaging of a preselected area, and specific properties of NFOS images as compared to SEM and conventional optical micrographs.

Sample I was chosen to demonstrate the outstanding resolution attainable with NFOS microscopy. The test object is a Ta film of 30-nm thickness with small circular holes of 100-nm diameter, kindly supplied by U. Ch. Fischer, MPI Göttingen, Federal Republic of Germany. The holes are shadow images of latex spheres dispersed on the glass slide during evaporation of the metal film. This sample provided the NFOS picture [**Figure 5(a)**] which is, we believe, the *highest-resolution optical micrograph ever produced.* The 100-nm holes are completely resolved. At the borders of the holes, one recognizes small imperfections such as peninsulae and other deviations from the expected circular shape. Two neighboring holes at the lower left can be clearly distinguished. Several tiny dark spots are also visible within the gray areas of the undisturbed film.

A corresponding scanning electron micrograph is shown in **Figure 5(b)**. The area depicted is not exactly the same as in the NFOS image. The random nature of the sample made an unequivocal identification of the scanned area impossible. However, it shows the same characteristic features: 100-nm holes and tiny protrusions of even smaller dimensions. The latter may be the origin of the fine dark spots in the NFOS picture.

The line scan [**Figure 5(c)**] corresponding to the NFOS micrograph gives a quantitative record of the transmitted intensity. The inset is shown in larger magnification in **Figure 5(d)**. Details recognizable in the micrograph and the line scan suggest that a resolution of 20 nm was achieved. When the same sample was observed with a conventional microscope, not the least structure could be seen. We therefore refrained from adding a conventional micrograph to Figure 5.

NFOS micrographs of the quality of Figure 5(a) are close to the resolution limit and cannot yet be routinely obtained. Optimum tip shape and aperture size as well as smooth sample surfaces are required to achieve this kind of performance. Another example of a high-resolution NFOS record is the inset to Figure 2 showing the border line of an opaque metal film on a glass substrate. Note the sharp rim of the dark bay and the small bright islands at the top.

NFOS records with lower resolution, say of the order of 50 to 100 nm, were obtained more routinely. In the next example, we compare medium-resolution NFOS scans with SEM and conventional optical micrographs of a preselected sample area.

Sample II is a transparent 400-nm-periodicity line-grating structure in a chromium film. An SEM micrograph of a particular corner of the structure is shown in **Figure 6(a)**. The conventional optical micrograph [**Figure 6(b)**] allows identification of the coarse features only, despite the use of immersion oil to maximize the numerical aperture of collimator and objective. The NFOS micrograph [**Figure 6(c)**] shows a much more detailed picture. The similarity to the SEM image is apparent, but typical differences can also be recognized: The bright traces on the left half of the NFOS scan are probably caused by protrusions on the sample surface, preventing optimally close scanning. As a result, erratic fluctuations of the intensity were observed. The degradation of the chromium film in the upper right corner of the inset of Figure 6(c) is hardly visible with the SEM [**Figure 6(d)**], whereas the same defect manifests itself as a bright distinct spot in the NFOS picture [**Figure 6(e)**]. Such differences are to be expected in view of the different imaging processes involved.

4. Outlook

The technique of NFOS is still in an early stage, with many possibilities for extensions and improvements. A sizable further increase in resolution is not to be expected, though, because of the finite skin depth of metals at optical frequencies.

Open questions that can be tackled with the present instrument are the response to phase objects, polarization properties of the transmitted radiation, color-picture capability, and presumably fluorescence microscopy. Reflection NFOS, one of the most important extensions, might be achieved by combination with Fischer's scheme [8]. The problem is to guide radiation to the aperture without feeding too much stray light into the observation microscope.

Another important extension is near-field scanning in the infrared range between 1 μm and 10 μm. A microscope with a resolution of 0.5 μm should be fairly easy to implement. Covering the so-called fingerprint region, the distribution of organic chemicals along a surface would show up with high chemical selectivity and positional resolution.

References

1. D. W. Pohl, "Optical Near-Field Scanning Microscope," European Patent Application No. 0112401, December 27, 1982.
2. D. W. Pohl, W. Denk, and M. Lanz, "Optical Stethoscopy: Image Recording with Resolution $\lambda/20$," *Appl. Phys. Lett.* **44**, 651 (1984).
3. U. Dürig, D. W. Pohl, and F. Rohner, "Near Field Optical Scanning Microscopy," *J. Appl. Phys.* **59**, 3318 (1986).
4. G. A. Massey, "Microscopy and Pattern Generation with Scanned Evanescent Waves," *Appl. Opt.* **23**, 658 (1984).
5. E. A. Ash and G. Nichols, "Super-Resolution Aperture Scanning Microscope," *Nature* **237**, 510 (1972).
6. A. Lewis, M. Isaacson, A. Murray, and A. Harootunian, "Scanning Optical Spectral Microscopy with 500 Å Spatial Resolution," *Biophys. J.* **41**, 405a (1983).
7. G. A. Massey, J. A. Davis, S. M. Katnik, and E. Omon, "Subwavelength Resolution Far-Infrared Microscopy," *Appl. Opt.* **24**, 1498 (1985).
8. U. Ch. Fischer, "Optical Characteristics of 0.1 μm Circular Apertures in a Metal Film as Light Sources for Ultramicroscopy," *J. Vac. Sci. Technol.* **33**, 386 (1985).
9. Piezo-Electric Products Inc., 212 Durham Ave., Metuchen, NJ 08840; Type R512P.

Received January 23, 1986; accepted for publication April 4, 1986

Urs Dürig *IBM Zurich Research Laboratory, Säumerstrasse 4, 8803 Rüschlikon, Switzerland.* Dr. Dürig received his Diploma in experimental physics from the Swiss Federal Institute of Technology (ETH), Zurich in 1979. He then became an assistant in the research group of Prof. W. Kaenzig in the Laboratory of Solid-State Physics of the ETH. He received the Ph.D. degree from the ETH in May 1984. Since then, he has been working on the near-field optical scanning (NFOS) microscope in the group of D. W. Pohl at the IBM Zurich Research Laboratory.

Dieter W. Pohl *IBM Zurich Research Laboratory, Säumerstrasse 4, 8803 Rüschlikon, Switzerland.* Dr. Pohl joined IBM in 1968 after receiving his Ph.D. with first-class honors from the Technical University of Munich, Federal Republic of Germany. In 1962, Dr. Pohl operated one of the first lasers in Europe during the investigations for his Diploma thesis. At IBM, he worked on problems of nonlinear optics and light scattering for several years. In 1982, he joined the IBM Zurich effort on STM and related techniques. He now heads a project oriented toward the study of materials of technological interest. He is the inventor of the near-field optical microscope, which exploits micromechanical principles developed for STM to obtain optical images with near-electron-microscopical resolution. Dr. Pohl is a member of the European, Swiss, and German physical societies.

Flavio Rohner *IBM Zurich Research Laboratory, Säumerstrasse 4, 8803 Rüschlikon, Switzerland.* On finishing his studies at the Swiss Federal Institute of Technology (ETH), Zurich, Mr. Rohner joined the IBM Zurich Research Laboratory in 1984. Since then he has specialized in the instrumental aspects of NFOS microscopy and sample preparation.